NH_4^+ triggers the release of astrocytic lactate via mitochondrial pyruvate shunting

Rodrigo Lerchundi[a,b], Ignacio Fernández-Moncada[a,b], Yasna Contreras-Baeza[a,b], Tamara Sotelo-Hitschfeld[a,b], Philipp Mächler[c,d], Matthias T. Wyss[c,d], Jillian Stobart[c,d], Felipe Baeza-Lehnert[a], Karin Alegría[a], Bruno Weber[c,d], and L. Felipe Barros[a,1]

[a]Biological Laboratory, Centro de Estudios Científicos, 5110466 Valdivia, Chile; [b]Universidad Austral de Chile, 5110566 Valdivia, Chile; [c]Institute of Pharmacology and Toxicology, University of Zurich, 8057 Zurich, Switzerland; and [d]Neuroscience Center Zurich, Eidgenössische Technische Hochschule (ETH), and University of Zurich, 8057 Zurich, Switzerland

Edited by Marcus E. Raichle, Washington University in St. Louis, St. Louis, MO, and approved July 29, 2015 (received for review April 28, 2015)

Neural activity is accompanied by a transient mismatch between local glucose and oxygen metabolism, a phenomenon of physiological and pathophysiological importance termed aerobic glycolysis. Previous studies have proposed glutamate and K^+ as the neuronal signals that trigger aerobic glycolysis in astrocytes. Here we used a panel of genetically encoded FRET sensors in vitro and in vivo to investigate the participation of NH_4^+, a by-product of catabolism that is also released by active neurons. Astrocytes in mixed cortical cultures responded to physiological levels of NH_4^+ with an acute rise in cytosolic lactate followed by lactate release into the extracellular space, as detected by a lactate-sniffer. An acute increase in astrocytic lactate was also observed in acute hippocampal slices exposed to NH_4^+ and in the somatosensory cortex of anesthetized mice in response to i.v. NH_4^+. Unexpectedly, NH_4^+ had no effect on astrocytic glucose consumption. Parallel measurements showed simultaneous cytosolic pyruvate accumulation and NADH depletion, suggesting the involvement of mitochondria. An inhibitor-stop technique confirmed a strong inhibition of mitochondrial pyruvate uptake that can be explained by mitochondrial matrix acidification. These results show that physiological NH_4^+ diverts the flux of pyruvate from mitochondria to lactate production and release. Considering that NH_4^+ is produced stoichiometrically with glutamate during excitatory neurotransmission, we propose that NH_4^+ behaves as an intercellular signal and that pyruvate shunting contributes to aerobic lactate production by astrocytes.

laconic | pyronic | peredox | FLII^{12}Pglu700μΔ6 | mitoSypHer

Brain tissue is almost exclusively energized by the oxidation of glucose. However, during neuronal activation, there is a larger increase in local glucose consumption relative to oxygen consumption (1). As this mismatch occurs in the presence of normal or augmented oxygen levels, it has been termed aerobic glycolysis, paralleling the signal detected by functional magnetic resonance imaging (2). Aerobic glycolysis and its associated lactate surge are causally linked to diverse functions of the brain in health and disease (3–10). Two signals are known to trigger aerobic glycolysis in brain tissue: glutamate and K^+, which are released by active neurons and stimulate glycolysis in astrocytes (11, 12).

Neurons produce as much NH_4^+ as they produce glutamate, both molecules being stoichiometrically linked in the glutamate-glutamine cycle (13). Brain tissue NH_4^+ increases within seconds of neural activation (14–16) and is quickly released to the interstitium (17, 18) to be captured by astrocytes through K^+ channels and transporters (19). It is well established that chronic exposure to pathological levels of NH_4^+ such as those observed during liver failure has a major impact on brain metabolism, but it is not known whether this molecule may affect energy metabolism at physiological levels, particularly within the time scale of synaptic transmission. A previous study showed a reversible rise in brain tissue lactate and cerebral blood flow within minutes of an i.v. infusion of NH_4^+. In view of this result, NH_4^+ was speculated to have signaling roles in the brain (20). The aim of the present work was to investigate this possibility.

Results

Increased Lactate Production and Release by Physiological NH_4^+. To investigate the acute effect of NH_4^+ on astrocytic metabolism, we chose 0.2 mM, a concentration within physiological levels in brain tissue (15, 21, 22). Experiments were carried out in cell cultures, in acute brain tissue slices and in the somatosensory cortex in vivo. First, the release of lactate by pure astrocytes in culture during a 1-min exposure to NH_4^+ was estimated using an enzymatic assay. Consistent with previous reports (20, 23), a significant increase in extracellular lactate was observed at 5 mM NH_4^+. However, the enzymatic assay was unable to detect significant lactate release at 0.2 or 0.5 mM NH_4^+ (Fig. 1*A*). To improve the sensitivity of detection, lactate was measured within cells using Laconic (24). All imaging of cultured astrocytes was performed on mixed cultures of astrocytes and neurons, in which astrocytes are better differentiated in terms of energy metabolism (25). Standard glucose and lactate concentrations in the superfusate were 1 and 0.5 mM, respectively. Exposure of astrocytes to 0.2 mM NH_4^+ induced a rapid and reversible increase in cytosolic lactate, a response that varied from cell to cell (Fig. 1*B*). The effect was reproducible (Fig. 1*C*) and dose dependent (Fig. 1 *D* and *E*). Cultured astrocytes are net lactate producers. To clarify whether the accumulation of lactate was due to increased production or impaired release, astrocytes were exposed to NH_4^+ in the presence of the monocarboxylate transporter (MCT) blocker AR-C155858 (26), which in these cells abrogates lactate transport (24). As shown in Fig. 1*F*, the increased rate of lactate accumulation in the presence of the MCT blocker demonstrates NH_4^+ stimulated lactate production. Lactate release was assessed independently by real-time estimation of lactate levels in the immediate vicinity of astrocytes using a lactate-sniffer HEK 293 cell (27). Seeded on a brain cell culture, lactate sniffers were observed to lie on top of the astrocytic monolayer (Fig. 1*G*). As

Significance

Aerobic glycolysis is important for synaptic growth, neuronal excitability, memory formation, and behavior and is also involved in neurodegeneration. Here we present evidence, obtained with novel optical tools, to show that NH_4^+ contributes to aerobic glycolysis by specifically inhibiting the mitochondrial consumption of pyruvate in astrocytes. NH_4^+, a waste product of excitatory neurotransmission, is therefore proposed to behave as an intercellular signal in brain tissue.

Author contributions: R.L., I.F.-M., Y.C.-B., T.S.-H., P.M., M.T.W., J.S., F.B.-L., B.W., and L.F.B. designed research; R.L., I.F.-M., Y.C.-B., T.S.-H., P.M., M.T.W., J.S., F.B.-L., and K.A. performed research; R.L., I.F.-M., Y.C.-B., T.S.-H., P.M., M.T.W., J.S., F.B.-L., K.A., B.W., and L.F.B. analyzed data; and R.L., B.W., and L.F.B. wrote the paper.

The authors declare no conflict of interest.

This article is a PNAS Direct Submission.

[1]To whom correspondence should be addressed. Email: fbarros@cecs.cl.

This article contains supporting information online at www.pnas.org/lookup/suppl/doi:10.1073/pnas.1508259112/-/DCSupplemental.

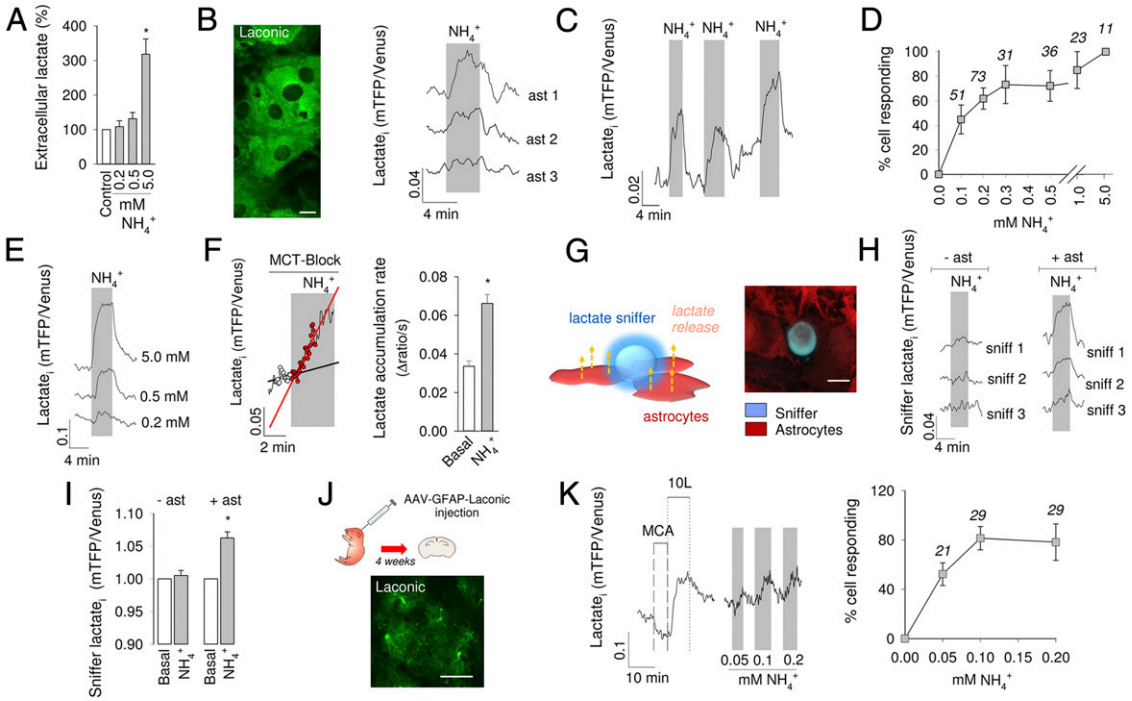

Fig. 1. NH_4^+ stimulates the production and release of lactate by astrocytes in vitro. (*A*) Extracellular lactate measurement with an enzymatic kit in pure astrocytic cultures. Cells were exposed for 1 min to 0.2, 0.5, or 5 mM NH_4^+. (*B*) (*Left*) Laconic expressed in the cytosol of astrocytes in culture. (Scale bar, 10 μm.) (*Right*) Effect of NH_4^+ on intracellular lactate is shown for 3 representative cells as the change of the mTFP/Venus ratio. (*C*) An astrocyte was exposed three times to 0.2 mM NH_4^+. (*D*) Dose dependence of the effect expressed as percentage of cells responding to NH_4^+ with an increase in lactate. Responding cells were distinguished from nonresponding cells by computing the average of five data points collected just before NH_4^+ exposure and the average of five data points at 3 min of exposure. The difference between the two values was considered significant if $P < 0.05$ (Mann-Whitney *u* test). The number of monitored cells is given. (*E*) Response of a single astrocyte to subsequent exposures to 0.2, 0.5, and 5 mM NH_4^+. (*F*) Astrocytes in glucose alone as energy substrate were first exposed to the MCT inhibitor AR-C155858 (1 μM) and 2 min later to 0.2 mM NH_4^+. Lines represent the rate of lactate accumulation before and during exposure to NH_4^+. Bars show averages. (*G*) (*Left*) Schematic representation of lactate sniffers above astrocytes. (*Right*) 3D confocal microscopy reconstruction of HEK 293 lactate sniffers (blue) and astrocytes loaded with Calcein orange (red). (*H*) Representative responses of sniffer cells exposed to 0.2 mM NH_4^+ in the absence and presence of astrocytes. (*I*) Bars show average changes in sniffer signal. (*J*) Protoplasmic astrocytes expressing Laconic in an acute hippocampal slice prepared 4 wk after AAV injection at P1. (Scale bar, 50 μm.) (*K*) (*Left*) Two-point calibration of Laconic with 50 mM monochloroacetate (MCA) and 10 mM lactate (10L), and response of a protoplasmic astrocyte to slice exposure to 0.05, 0.1, and 0.2 mM NH_4^+. (*Right*) Dose dependence of the effect expressed as percentage of cells responding to 0.2 mM NH_4^+ with an increase in lactate. Responding cells were identified as detailed in *D*. The number of monitored cells is given. $*P < 0.05$.

shown in Fig. 1 *H* and *I*, exposure of the cultures to NH_4^+ resulted in a rapid increase in sniffer signal that was variable in amplitude and reverted to baseline after NH_4^+ withdrawal. These results show that astrocytes increase their production and release of lactate within seconds of exposure to physiological levels of NH_4^+.

To verify if the response of astrocytes to NH_4^+ is detectable in brain tissue, lactate was measured in protoplasmic astrocytes of the hippocampus. For this purpose, a recombinant adeno-associated virus coding for Laconic under the short gfaABC$_1$D promoter was stereotactically injected into the brain of neonatal mice. After 4–5 wk, brain slices were prepared, and FRET measurements were made (Fig. 1*J*). Imaged in tissue slices, the sensor behaved as expected, with a decrease in signal on transacceleration of lactate export with the nonmetabolized MCT substrate monochloroacetate and an increase during exposure to 10 mM lactate (24). Addition of NH_4^+ to the slice caused a rapid increase in lactate in protoplasmic astrocytes, a response that could be detected even at 0.05 mM NH_4^+ (Fig. 1*K*). To approach astrocytic lactate in vivo, Laconic was expressed in astrocytes of the primary somatosensory cortex of adult mice and then imaged under anesthesia through a cranial window using two-photon microscopy (Fig. 2*A*). An i.v. bolus injection of NH_4^+ (2.5 mmol/kg body weight) provoked a quick rise in astrocytic lactate (Fig. 2*B*), followed by a rise in extracellular lactate, as detected by an enzyme-based microelectrode inserted into the brain tissue (Fig. 2*C*). Parallel measurements showed no apparent effects of the NH_4^+ bolus infusion on blood lactate levels (Fig. 2*D*), demonstrating that the changes detected in the brain were originated locally. Less NH_4^+ was also capable of increasing astrocytic lactate, with a lowest effective dose of 0.63 mmol/ kg (Fig. 2*E*). Considering that a bolus of 2.5 mmol/kg increased brain tissue NH_4^+ by 0.7 mM (20), the 0.63 mmol/kg bolus should have increased brain NH_4^+ by 0.17 mM. This calculated value, which is close to the physiological range, is probably an overestimate as it does not take into account NH_4^+ clearance by peripheral tissues and by astrocytes. Aerobic glycolysis may be triggered by stimulation of astrocytic glycolysis, such as that observed in response to glutamate or to high K^+ (11, 12). To assess glycolysis as a possible target for NH_4^+, astrocytic glucose was measured using the genetically encoded glucose nanosensor FLII^{12}Pglu700μΔ6 (28). As shown in Fig. S1, exposure to physiological NH_4^+ levels had no apparent effect on cytosolic glucose concentration nor on the rate of glucose consumption measured with a transport block protocol (29). We conclude that physiological NH_4^+ does not stimulate glucose consumption in astrocytes.

Mitochondrial Flux Inhibition by Physiological NH_4^+. In lactate producers like astrocytes, most NADH is produced in glycolysis. Measurements with the genetically encoded fluorescent nanosensor Peredox (30) showed a decrease in cytosolic NADH in response to NH_4^+ (Fig. 3*A*), a result that is consistent with the lack of effect of NH_4^+ on glucose consumption and that also rules out glycogen as a putative source of lactate. Thus, we focused on

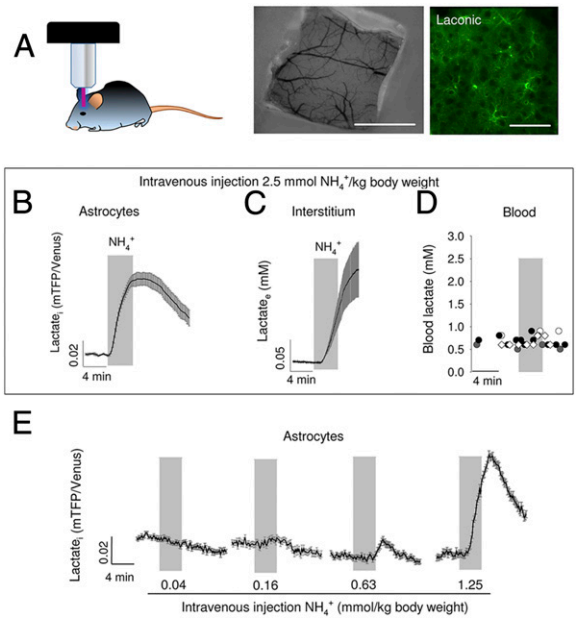

Fig. 2. NH_4^+ increases astrocytic lactate in vivo. (*A*) Schematic representation of an in vivo experiment. (*Left*) Anesthetized mouse previously injected with AAV9-GFAP-Laconic is positioned in the two-photon microscope setup for measurement of astrocytic lactate. (*Center*) Cranial window exposing the somatosensory cortex. (Scale bar, 1 mm.) (*Right*) Protoplasmic astrocytes expressing Laconic in the somatosensory cortex, layer II/III. (Scale bar, 50 μm.) A bolus of NH_4^+ (2.5 mmol/kg body weight) was injected i.v. while monitoring astrocytic lactate with Laconic (*B*), extracellular lactate with an inserted biosensor (*C*), or blood lactate with an enzymatic assay (*D*). Symbols in *D* represent data from four separate experiments. (*E*) Response of astrocytic lactate to sequential i.v. injections of increasing doses of NH_4^+.

mitochondrial inhibition as the possible mechanism for the lactate surge. Measurements with the FRET nanosensor Pyronic (31) supported this hypothesis by showing a rapid increase of cytosolic pyruvate in response to NH_4^+, which could be observed even at 0.05 mM (Fig. 3*B*). Next, mitochondrial pyruvate consumption was monitored using a transport block protocol (31). Briefly, astrocytes were first incubated with pyruvate alone as energy substrate and then were exposed to a mixture of surface pyruvate transport blockers, a condition under which the rate of cytosolic pyruvate depletion represents the rate of mitochondrial pyruvate consumption. In our culture conditions, the uptake of pyruvate is partly mediated by a pathway sensitive to AR-C155858 and by a pathway sensitive to probenecid. As shown in Fig. 3*C*, NH_4^+ markedly decreased mitochondrial pyruvate consumption. To further characterize the dynamics of mitochondrial inhibition, cells were simultaneously exposed to NH_4^+ and pyruvate transport blockers during high-frequency data acquisition. During the first seconds of exposure, the rate of pyruvate depletion was similar to that observed in the absence of NH_4^+, but then the depletion came to a stop and pyruvate levels began to recover. A numerical model of pyruvate dynamics could be fitted to the data, indicating that NH_4^+ inhibited mitochondrial pyruvate uptake by 93%, with a delay of 30 s between surface transport block and mitochondrial inhibition (Fig. 3*D*). The resulting accumulation of pyruvate in the cytosol pushes the near-equilibrium LDH reaction toward NADH use and lactate production, thus accounting for the observed decrease in cytosolic NADH.

Mechanism of Mitochondrial Pyruvate Uptake Inhibition by NH_4^+. A robust cytosolic acidification was obtained with supraphysiological NH_4^+ (Fig. 3*E*), confirming that ammonium enters astrocytes mostly in the protonated form, a process known to be mediated by K^+ channels and transporters (19, 22). Exposure of astrocytes to physiological NH_4^+ caused a significant acidification of the mitochondrial matrix, as estimated with MitoSypHer, a genetically-encoded pH sensor (Fig. 3*F*). The mitochondrial acidification suggests that ammonium enters astrocytic mitochondria in the protonated form. We could not find information about the mechanisms of mitochondrial NH_4^+ transport in astrocytes. Preferential NH_4^+ over NH_3 uptake has previously been reported in liver mitochondria (32). Of note, although NH_3 is a gas, it diffusivity through biological membranes can be low, as reported in kidney cells (33). In contrast, physiological NH_4^+ did not acidify the cytosol to a significant extent (Fig. 3*E*). The absence of cytosolic acidification by low levels of ammonium is consistent with the higher pH and lower buffering capacity of the mitochondrial matrix relative to the cytosol (34), compounded by muffling from the high levels of cytosolic bicarbonate and carbonic anhydrase present in astrocytic cytosol (35). The uptake of pyruvate by mitochondria is mediated by the mitochondrial pyruvate carrier (MPC), which is an H^+-pyruvate cotransporter (36, 37). Therefore, the driving force for pyruvate uptake depends on the difference between the H^+ concentration in the cytosol and that in the more alkaline mitochondrial matrix (38). Because the MPC cotransports pyruvate with an H^+, the acidification of mitochondria by physiological NH_4^+ provides an explanation for the inhibition of pyruvate uptake by mitochondria. After entering mitochondria, most of the pyruvate is metabolized via the Krebs cycle. This pathway may be inhibited by NH_3 at α-ketoglutarate dehydrogenase (21), a possible downstream target for NH_4^+ after deprotonation. NH_4^+ had no apparent effect on mitochondrial membrane potential (Fig. 3*G*). A stable mitochondrial potential in the face of matrix acidification has been previously ascribed to Ca^{2+} efflux (39), but we could not find a detectable increase in cytosolic Ca^{2+} in astrocytes exposed to NH_4^+ (Fig. S2). An alternative explanation for the constancy of mitochondrial potential may be inhibition of ATP synthase mediated by the H^+-sensitive modulator IF1 (40).

Discussion

This article describes a previously unidentified mechanism of aerobic glycolysis. We found that physiological levels of NH_4^+ induce a rapid and reversible increase in lactate production and release by astrocytes, a robust phenomenon observed in cultured cells, brain tissue slices, and in the somatosensory cortex in vivo. In contrast to the metabolic roles of glutamate and K^+, the NH_4^+-dependent lactate surge was not due to glycolytic stimulation but to pyruvate shunting, explained by acidification of the mitochondrial matrix. As NH_4^+ is produced by neurons in an activity-dependent manner, the present mechanism suggests that NH_4^+ diverts lactate from astrocytes to neurons (Fig. 4).

NH_4^+ as a Marker for Neurotransmission. Astrocytes capture glutamate released during excitatory neurotransmission and send it back to neurons in the form of glutamine. Within neurons, glutamine is reconverted to glutamate with the stoichiometric production of NH_4^+ (13). The physiological concentration of NH_4^+ in brain tissue of several species has been estimated at about 0.2 mM (15, 21), with a more recent 0.45 mM measured in mouse brain interstitium with a double barreled electrode (22). An increase in nervous tissue NH_4^+ during neural activity has been reported in several animal models, including frog sciatic nerve (14), rat brain slices (15), and slices of the bee retina (17). Using a rapid freezing technique, a transient increase in brain tissue NH_4^+ was detected within 5 s of rat paw stimulation (16). It is not clear whether NH_4^+ is released together with glutamate during synaptic vesicle fusion (41) or alternatively through NH_4^+-permeable ion channels (42). NH_4^+ is rapidly captured by astrocytes via several pathways including K^+ channels and transporters (19, 22). Nitrogen may also be shuttled from neurons to astrocytes as

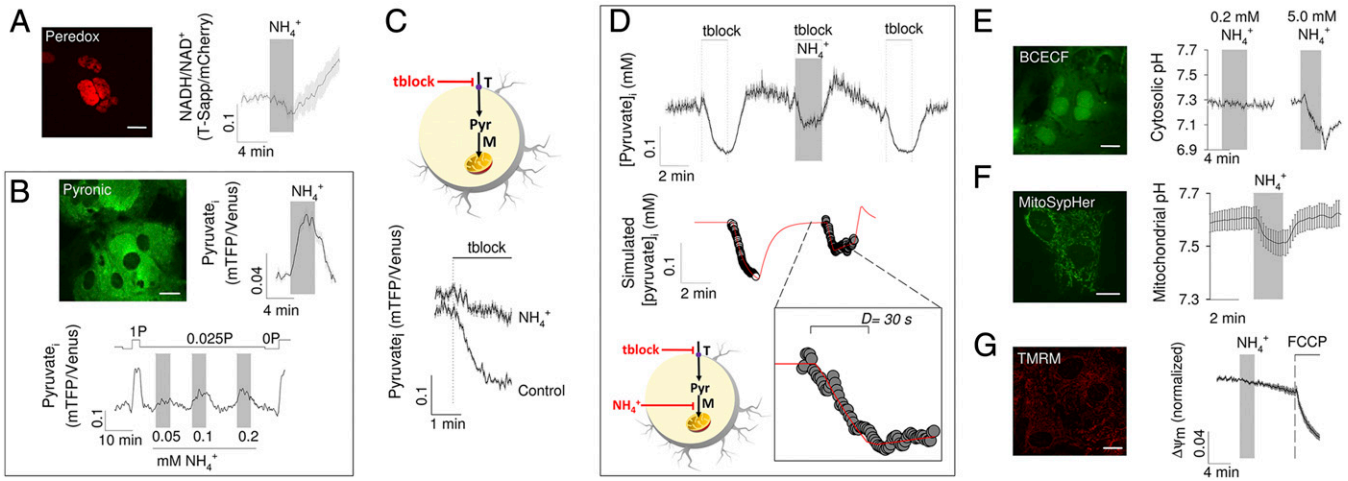

Fig. 3. Mitochondrial inhibition induced by NH_4^+. (*A*) Cultured astrocytes expressing the NADH/NAD$^+$ nanosensor Peredox in the nucleus. (Scale bar, 10 μm.) The graph shows the effect of 0.2 mM NH_4^+ on the NADH/NAD$^+$ ratio. (*B*) Cultured astrocytes expressing the pyruvate nanosensor Pyronic. (Scale bar, 10 μm.) The graph in the middle shows the effect of 0.2 mM NH_4^+ on astrocytic pyruvate. (*Right*) Response of a single astrocyte to subsequent exposures to 0.05, 0.1, and 0.2 mM NH_4^+. Pyruvate in the superfusate (P) was set at 0.025 mM during the stimulations or 0 and 1 mM for calibration purposes. (*C*) (*Upper*) Schematic representation of the method that estimates mitochondrial pyruvate consumption by inhibiting surface pyruvate transport (T) with 100 nM AR-C155858 and 1 mM probenecid (tblock). (*Lower*) Mitochondrial pyruvate consumption in cells that had been exposed for 3 min to 0.2 mM NH_4^+ and their controls. (*D*) (*Upper*) Surface pyruvate transport was blocked in the absence and presence of 0.2 mM NH_4^+. (*Lower*) Numerical model represented in the schematic was fitted (red line) to the pyruvate data (symbols) as described in the *SI Text*. (*Inset*) Delay in the onset of the NH_4^+ effect. (*E*) Effects of 0.2 and 5.0 mM NH_4^+ on astrocytic pH, estimated with BCECF. (*F*) Effect of 0.2 NH_4^+ on mitochondrial pH, estimated with mitoSypHer. (*G*) Effects of 0.2 NH_4^+ and 1 μM FCCP on mitochondrial membrane potential estimated with TMRM. (Scale bars, 10 μm.)

amino acids, but the extent of this indirect pathway seems to be less significant than direct transfer as NH_4^+ (18).

Mechanism of Lactate Production by NH_4^+. We observed that NH_4^+ acutely stimulated the production and release of lactate by astrocytes without affecting glycolysis. The phenomenon was detected even at 0.05 mM and coincided with a strong inhibition of pyruvate uptake by mitochondria. There was a coincidental decrease in cytosolic NADH, consistent with pyruvate to lactate conversion. NH_4^+ caused an acute acidification of the mitochondrial matrix but no detectable changes in cytosolic pH. The uptake of pyruvate by mitochondria is mediated by the H^+-coupled MPC (36, 37), and therefore the reduction of the transmitochondrial pH gradient by NH_4^+ provides a parsimonious explanation for the reduced uptake of pyruvate. There is increasing evidence that mitochondrial pH plays important physiological and pathological roles (43); for example, a recent study in astrocytes showed that glutamate inhibited oxygen consumption, a phenomenon ascribed to cytosolic acidification leading to mitochondrial acidification (34).

NH_4^+ Is a Signal for Aerobic Glycolysis. The control, by neurons, of astrocytic lactate release appears to involve several mechanisms acting within different temporal domains. In the short term (seconds), glutamate stimulates the glucose transporter GLUT1 via Na^+ and Ca^{2+} transients mediated by the Na^+-glutamate cotransporter (44, 45). Acting in parallel, K^+ stimulates glycolysis via the Na^+-HCO_3^- cotransporter NBCe1 (12, 46) and also opens a lactate permeable ion channel at the cell surface (27). By suppressing the uptake of pyruvate by astrocytic mitochondria within seconds, NH_4^+ adds an additional strategy for short-term induction of aerobic glycolysis. Acting on different targets, the three signals are likely to be synergic. The production of lactate by astrocytes is also stimulated by neuronal signals in the long term (minutes). Glutamate activates glycolysis via the Na^+-glutamate cotransporter (11, 12) and K^+ stimulates glycogen degradation via the HCO_3^--sensitive soluble adenylyl cyclase (47). Also within minutes, nitric oxide has been shown to stimulate astrocytic glycolysis through inhibition of cytochrome *c* oxidase leading to activation of 5′-AMP–activated protein kinase and PFKFB3 (48). It seems likely that NH_4^+ may also have long-term roles in the control of astrocytic glycolysis and similar mechanisms could be present in other glial cells. For example, retinal Müller cells have been shown to increase their production of lactate in response to NH_4^+, but only in the presence of glutamate (49). Cooperativity might also help to explain the present observation that astrocytes in brain slices, likely exposed to some glutamate, were found to be more sensitive to NH_4^+ than astrocytes in culture. Given the emerging importance of aerobic glycolysis and lactate for diverse

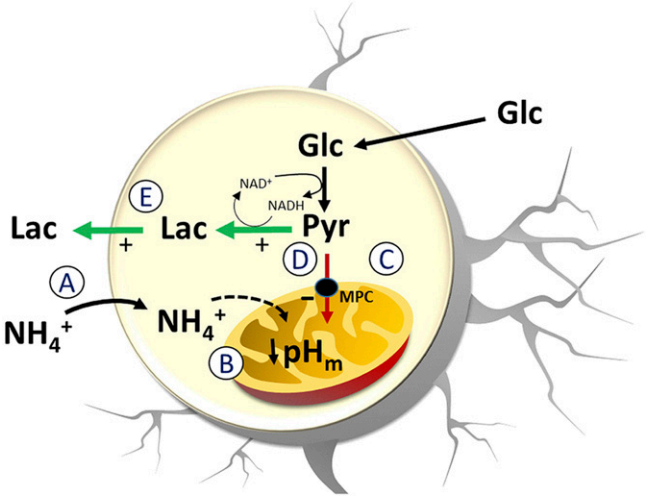

Fig. 4. Astrocytic lactate release in response to NH_4^+. The release of lactate by astrocytes exposed to NH_4^+ is explained by the following sequence of events. (*A*) NH_4^+ uptake by astrocytes through K^+ channels and transporters. (*B*) NH_4^+ entry into mitochondria leading to acidification of the mitochondrial matrix. (*C*) Inhibition of the H^+-coupled MPC. (*D*) Accumulation of pyruvate in the cytosol causing lactate accumulation and NADH depletion. (*E*) Increased lactate release.

local and higher functions of the brain (3–10, 50–55), we hope that the present findings will stimulate research on the physiological aspects of NH_4^+, particularly mitochondrial transport and neuronal release.

Materials and Methods

Standard reagents and inhibitors were acquired from Sigma or Merck. AR-C155858 was purchased from Haoyuan Chemexpress. The sensors FLII^{12}Pglu700μΔ6, Peredox, Laconic, Pyronic, and MitoSypHer are available from Addgene (www.addgene.org). Ad Laconic, Ad Pyronic, and Ad FLII^{12}Pglu700μΔ6 (serotype 5) were custom made by Vector Biolabs. The adeno-associated virus (AAV9) expressing Laconic under the control of the short gfaABC1D promoter was generated at the École Polytechnique Fédérale de Lausanne. Design, production, and titration of the AAV9 vector for transgene expression in astrocytes have been described previously (56). Fluo-4 AM, 2,7-bis-(2-carboxyethyl)-5-(and-6)-carboxyfluorescein (BCECF) AM, tetramethyl rhodamine methyl ester (TMRM), and Calcein AM were from Invitrogen. All NH_4^+ application were in the form of NH_4Cl. At pH 7.4 and 23 °C, 99% is in the ionized form (NH_4^+), and 1% is in the neutral form (NH_3).

Animals and Brain Cell Culture. All animal procedures for the in vitro experiments were approved by the Institutional Animal Care and Use Committee of the Centro de Estudios Científicos. Animals used for primary cultures and brain slices were mixed F1 male mice (C57BL/6J × CBA/J), kept in an animal room under SPF conditions at a room temperature of 20 ± 2 °C, in a 12/12-h light/dark cycle and with free access to water and food. Procedures for in vivo experiments were approved by the local veterinary authorities, conforming to the guidelines of the Swiss Animal Protection Law, Veterinary Office, Canton Zurich (Act of Animal Protection 16 December 2005 and Animal Protection Ordinance 23 April 2008). WT mice (C57BL/6J; Harlan Laboratories) 10 wk of age and with a body weight of 20 g were housed in single cages, with free access to water and food. Mixed brain cell primary cultures were prepared as detailed previously (46). To measure lactate release with an enzymatic method, pure astrocytic cultures were obtained by subculturing mixed cultures at day 14. After another 7 d in 24-well plates, cultures were exposed to experimental conditions in a 95% air/5% CO_2-gassed culture saline buffer (CSF) composed of (mM) 112 NaCl, 3 KCl, 1.25 $CaCl_2$, 1.25 $MgCl_2$, 2 glucose, 10 Hepes, and 24 $NaHCO_3$, pH 7.4, at room temperature. Extracellular lactate was measured using a fluorometric assay kit according to the manufacturer´s instructions (BioVision). For FRET sensor expression, cultures were exposed to 5×10^6 PFU of Ad Laconic, Ad Pyronic, or Ad FLII^{12}Pglu700μΔ6 and studied after 48 h (culture day 8–10). For plasmid expression of Peredox and mitoSypHer, cells were transfected using Lipofectamine 2000 or 3000 (Gibco) and studied after 48 h (culture day 8–10). The cytosolic and nuclear versions of Peredox responded similarly to NH_4^+, as expected from unrestricted movement of NADH and NAD^+ through the nuclear pore (30). However, the expression of nuclear Peredox was much stronger. Thus, we chose to illustrate NADH dynamics using nuclear Peredox. To generate lactate sniffers (27), HEK293 cells were first transfected with Laconic. After 24 h, the cells were detached with trypsin for 2 min, washed three times, and seeded on top of a mixed brain cell culture. The coculture was maintained with Neurobasal medium for 12–24 h until imaging.

Hippocampal Slices. Neonatal mice (postnatal days 1–2) were removed from the mother and anesthetized by hypothermia for 8 min. Animals were positioned on a stereotactic stage (57) and injected with 1 μL AAV9-GFAP-Laconic directly through the skull using a Fusion 100 Syringe Pump (Chemyx). After injection, animals were positioned on a temperate bed until recovery and returned to the mother. Four weeks after AAV injection, animals were killed by cervical dislocation, and 200-μm-thick coronal brain sections were prepared as described (58).

In Vivo Two-Photon Microscopy of Somatosensory Cortex. The protocol for in vivo determination of astrocytic lactate with Laconic has been detailed elsewhere (27). In brief, animals were anesthetized with an intraperitoneally injected mixture of fentanyl (0.05 mg/kg body weight; Sintenyl, Sintetica), midazolam (5 mg/kg body weight; Dormicum, Roche), and medetomidine (0.5 mg/kg body weight; Domitor, Orion Pharma) and again after 50 min with midazolam only (5 mg/kg body weight). The head was fixed in a stereotactic apparatus, and the eyes were kept wet with an ointment (vitamin A eye cream; Bausch & Lomb). A 4 × 4-mm craniotomy was drilled using a dental drill, and 75 nL AAV9-GFAP-Laconic (titer 3.1×10^{12} vg/mL) was injected into the primary somatosensory cortex. A square coverslip (3 × 3 mm; UQG Optics Ltd.) was lightly pressed on the exposed brain and fixed with dental cement to the skull. A bonding agent (Gluma Comfort Bond; Heraeus Kulzer) was applied to the cleaned skull and was polymerized with a handheld blue light source (600 mW/cm^2; Demetron LC, Kerr Corporation). The open skin was treated with an antibiotic ointment (Cicatrex; Janssen-Cilag AG) and closed with acrylic glue (Histoacryl; B. Braun). After surgery, the animals were kept warm and provided with analgesics (Novaminsulfon, 50%; Sintetica), and the antibiotic enrofloxacin was added to the drinking water (200 mg/L drinking water; Baytril, Bayer). For in vivo lactate measurements, mice were imaged with a custom-built two-photon laser-scanning microscope using a tunable pulsed (Mai Tai eHP DS system; Spectra-Physics) at a wavelength of 870 nm. The animals were head fixed and kept under anesthesia, as described above. Body temperature was kept constant with a feedback-controlled heating pad (37 °C; Harvard Apparatus). Extracellular lactate measurements were performed with the commercially available recording system from Pinnacle Technology. Mice were fixed in a stereotactic frame under anesthesia (isoflurane 1.5%; Abbott), the skull was opened with a dental drill, and a guide cannula (Part 7032; Pinnacle Technology) was implanted into the primary somatosensory cortex (A/P +1.41, M/L −2.8, D/V −1.0) and fixed with dental cement to an anchor screw (Part 8209; Pinnacle Technology). After a recovery period of 2 wk, the precalibrated lactate sensor was inserted into the guide cannula. A tail vein catheter was created for saline, lactate, and pyruvate infusions. Recording was started 1 h after signal stabilization. For blood lactate level measurements, the femoral artery was exposed and cannulated with fine bore polyethylene tubing (0.28 mm ID, 0.61 mm OD, Portex; Smiths Medical). Blood drops were removed from the cannula, and every fourth drop was used for an enzymatic lactate assay (Lactate Pro-2; Arkray). After each blood sample analysis, the tubing was rinsed with heparinized (50 IU/mL) 0.9% saline solution.

In Vitro Fluorescence Imaging. Detailed protocols for the use of the fluorescent sensors are available (59–62). Cells and slices were imaged with an upright Olympus FV1000 confocal microscope and a 440-nm solid-state laser. Alternatively, cells were imaged with Olympus IX70 or BX51 microscopes equipped with Cairn Research monochromators and Optosplits and either a Hamamatsu Orca or Rollera camera. Cells were superfused at 1 mL/min (chamber volume, 0.3 mL) at room temperature (22–24 °C): Cultures were superfused with a 95% air/5% CO_2-gassed CSF (1 mM glucose and 0.5 mM NaLactate), and tissue slices with a 95% O_2/5% CO_2-gassed solution composed of (mM) 126 NaCl, 3 KCl, 1.25 NaH_2PO_4, 1.25 $CaCl_2$, 1.25 $MgCl_2$, 10 glucose, and 26 $NaHCO_3$, at pH 7.4. Cell cultures were imaged approximately 30 min after Neurobasal removal; Typical time between animal killing and slice imaging was 2 h. Masked ratio images were generated from background-subtracted images using ImageJ software. Fluo4 was ester loaded at 4 μM for 15 min. BCECF was ester loaded at 0.1 μM for 3–4 min. Calcein orange was ester loaded at 1 μM for 30 min. BCECF and mitoSypHer were calibrated by exposing the cultures to different pH in the presence of 10 μg/mL nigericin and 20 μg/mL gramicidin in an intracellular buffer. The permeabilization procedure shifted the mitoSypHer signal, and therefore baseline mitochondrial pH was assumed to be 7.6 (34). For mitochondrial membrane potential imaging the cultures were loaded with the fluorescent dye TMRM for 30 min at 37 °C.

Data Presentation and Statistical Analysis: Line traces without errors represent individual cells. Traces with error bars correspond to mean ± SEM of eight or more cells ($n \geq 3$ experiments). Differences between two groups were evaluated with the Student *t* test or the Mann-Whitney *u* test, and differences between more groups were evaluated with the Kruskal–Wallis one-way ANOVA on ranks followed by Dunn´s test. $P < 0.05$ was considered significant. The computer simulation of pyruvate dynamics is described in *SI Text*.

ACKNOWLEDGMENTS. We thank Christine Rose for helpful suggestion and Karen Everett for critical reading of the manuscript. This research was partly funded by Fondecyt Grant 1130095 (to L.F.B.). B.W. is partly supported by the Swiss National Science Foundation and the Clinical Research Priority Program of the University of Zurich on Molecular Imaging. The Centro de Estudios Científicos is funded by the Chilean Government through the Centers of Excellence Basal Financing Program of the Comisión Nacional de Investigación Científica y Tecnológica (CONICYT).

1. Fox PT, Raichle ME, Mintun MA, Dence C (1988) Nonoxidative glucose consumption during focal physiologic neural activity. *Science* 241(4864):462–464.
2. Raichle ME, Mintun MA (2006) Brain work and brain imaging. *Annu Rev Neurosci* 29: 449–476.
3. Mintun MA, Vlassenko AG, Rundle MM, Raichle ME (2004) Increased lactate/pyruvate ratio augments blood flow in physiologically activated human brain. *Proc Natl Acad Sci USA* 101(2):659–664.
4. Wyss MT, Jolivet R, Buck A, Magistretti PJ, Weber B (2011) In vivo evidence for lactate as a neuronal energy source. *J Neurosci* 31(20):7477–7485.
5. Suzuki A, et al. (2011) Astrocyte-neuron lactate transport is required for long-term memory formation. *Cell* 144(5):810–823.
6. Goyal MS, Hawrylycz M, Miller JA, Snyder AZ, Raichle ME (2014) Aerobic glycolysis in the human brain is associated with development and neotenous gene expression. *Cell Metab* 19(1):49–57.
7. Barros LF (2013) Metabolic signaling by lactate in the brain. *Trends Neurosci* 36(7): 396–404.
8. Barros LF, Sierralta J, Weber B (2015) How doth the little busy bee: Unexpected metabolism. *Trends Neurosci* 38(1):1–2.
9. Chandrasekaran S, et al. (2015) Aggression is associated with aerobic glycolysis in the honey bee brain(1). *Genes Brain Behav* 14(2):158–166.
10. Bero AW, et al. (2011) Neuronal activity regulates the regional vulnerability to amyloid-β deposition. *Nat Neurosci* 14(6):750–756.
11. Pellerin L, Magistretti PJ (1994) Glutamate uptake into astrocytes stimulates aerobic glycolysis: A mechanism coupling neuronal activity to glucose utilization. *Proc Natl Acad Sci USA* 91(22):10625–10629.
12. Bittner CX, et al. (2011) Fast and reversible stimulation of astrocytic glycolysis by K^+ and a delayed and persistent effect of glutamate. *J Neurosci* 31(12):4709–4713.
13. Schousboe A, Bak LK, Waagepetersen HS (2013) Astrocytic Control of Biosynthesis and Turnover of the Neurotransmitters Glutamate and GABA. *Front Endocrinol (Lausanne)* 4:102.
14. Tashiro S (1922) Studies on alkaligenesis in tissues. *Am J Physiol* 60:519–543.
15. Richter D, Dawson RM (1948) The ammonia and glutamine content of the brain. *J Biol Chem* 176(3):1199–1210.
16. Tsukada Y, Takagaki G, Sugimoto S, Hirano S (1958) Changes in the ammonia and glutamine content of the rat brain induced by electric shock. *J Neurochem* 2(4): 295–303.
17. Coles JA, Marcaggi P, Véga C, Cotillon N (1996) Effects of photoreceptor metabolism on interstitial and glial cell pH in bee retina: Evidence of a role for NH4+. *J Physiol* 495(Pt 2):305–318.
18. Rothman DL, De Feyter HM, Maciejewski PK, Behar KL (2012) Is there in vivo evidence for amino acid shuttles carrying ammonia from neurons to astrocytes? *Neurochem Res* 37(11):2597–2612.
19. Kelly T, Rose CR (2010) Ammonium influx pathways into astrocytes and neurones of hippocampal slices. *J Neurochem* 115(5):1123–1136.
20. Provent P, et al. (2007) The ammonium-induced increase in rat brain lactate concentration is rapid and reversible and is compatible with trafficking and signaling roles for ammonium. *J Cereb Blood Flow Metab* 27(11):1830–1840.
21. Cooper AJ, Plum F (1987) Biochemistry and physiology of brain ammonia. *Physiol Rev* 67(2):440–519.
22. Rangroo Thrane V, et al. (2013) Ammonia triggers neuronal disinhibition and seizures by impairing astrocyte potassium buffering. *Nat Med* 19(12):1643–1648.
23. Kala G, Hertz L (2005) Ammonia effects on pyruvate/lactate production in astrocytes–interaction with glutamate. *Neurochem Int* 47(1-2):4–12.
24. San Martín A, et al. (2013) A genetically encoded FRET lactate sensor and its use to detect the Warburg effect in single cancer cells. *PLoS One* 8(2):e57712.
25. Mamczur P, et al. (2015) Astrocyte-neuron crosstalk regulates the expression and subcellular localization of carbohydrate metabolism enzymes. *Glia* 63(2):328–340.
26. Ovens MJ, Davies AJ, Wilson MC, Murray CM, Halestrap AP (2010) AR-C155858 is a potent inhibitor of monocarboxylate transporters MCT1 and MCT2 that binds to an intracellular site involving transmembrane helices 7-10. *Biochem J* 425(3):523–530.
27. Sotelo-Hitschfeld T, et al. (2015) Channel-mediated lactate release by K^+-stimulated astrocytes. *J Neurosci* 35(10):4168–4178.
28. Takanaga H, Chaudhuri B, Frommer WB (2008) GLUT1 and GLUT9 as major contributors to glucose influx in HepG2 cells identified by a high sensitivity intramolecular FRET glucose sensor. *Biochim Biophys Acta* 1778(4):1091–1099.
29. Bittner CX, et al. (2010) High resolution measurement of the glycolytic rate. *Front Neuroenergetics* 2:1–11.
30. Hung YP, Albeck JG, Tantama M, Yellen G (2011) Imaging cytosolic NADH-NAD(+) redox state with a genetically encoded fluorescent biosensor. *Cell Metab* 14(4): 545–554.
31. San Martín A, et al. (2014) Imaging mitochondrial flux in single cells with a FRET sensor for pyruvate. *PLoS One* 9(1):e85780.
32. Gutiérrez C, Beaty G, López-Vancell R, Estrada S (1987) Mechanism of ammonium translocation in rat liver mitochondria. Finger-printing of the translocator. *Acta Physiol Pharmacol Latinoam* 37(2):257–275.
33. Kikeri D, Sun A, Zeidel ML, Hebert SC (1989) Cell membranes impermeable to NH3. *Nature* 339(6224):478–480.
34. Azarias G, et al. (2011) Glutamate transport decreases mitochondrial pH and modulates oxidative metabolism in astrocytes. *J Neurosci* 31(10):3550–3559.
35. Deitmer JW, Rose CR (1996) pH regulation and proton signalling by glial cells. *Prog Neurobiol* 48(2):73–103.
36. Bricker DK, et al. (2012) A mitochondrial pyruvate carrier required for pyruvate uptake in yeast, Drosophila, and humans. *Science* 337(6090):96–100.
37. Herzig S, et al. (2012) Identification and functional expression of the mitochondrial pyruvate carrier. *Science* 337(6090):93–96.
38. Poburko D, Demaurex N (2012) Regulation of the mitochondrial proton gradient by cytosolic Ca^{2+} signals. *Pflugers Arch* 464(1):19–26.
39. Perry SW, Norman JP, Barbieri J, Brown EB, Gelbard HA (2011) Mitochondrial membrane potential probes and the proton gradient: A practical usage guide. *Biotechniques* 50(2): 98–115.
40. Campanella M, Parker N, Tan CH, Hall AM, Duchen MR (2009) IF(1): Setting the pace of the F(1)F(o)-ATP synthase. *Trends Biochem Sci* 34(7):343–350.
41. Marcaggi P (2006) An ammonium flux from neurons to glial cells. *Proc Physiol Soc* 3:SA16.
42. Marcaggi P, Coles JA (2001) Ammonium in nervous tissue: Transport across cell membranes, fluxes from neurons to glial cells, and role in signalling. *Prog Neurobiol* 64(2):157–183.
43. Santo-Domingo J, Demaurex N (2012) Perspectives on: SGP symposium on mitochondrial physiology and medicine: The renaissance of mitochondrial pH. *J Gen Physiol* 139(6):415–423.
44. Loaiza A, Porras OH, Barros LF (2003) Glutamate triggers rapid glucose transport stimulation in astrocytes as evidenced by real-time confocal microscopy. *J Neurosci* 23(19):7337–7342.
45. Porras OH, Ruminot I, Loaiza A, Barros LF (2008) Na(+)-Ca(2+) cosignaling in the stimulation of the glucose transporter GLUT1 in cultured astrocytes. *Glia* 56(1):59–68.
46. Ruminot I, et al. (2011) NBCe1 mediates the acute stimulation of astrocytic glycolysis by extracellular K^+. *J Neurosci* 31(40):14264–14271.
47. Choi HB, et al. (2012) Metabolic communication between astrocytes and neurons via bicarbonate-responsive soluble adenylyl cyclase. *Neuron* 75(6):1094–1104.
48. Almeida A, Moncada S, Bolaños JP (2004) Nitric oxide switches on glycolysis through the AMP protein kinase and 6-phosphofructo-2-kinase pathway. *Nat Cell Biol* 6(1): 45–51.
49. Poitry S, Poitry-Yamate C, Ueberfeld J, MacLeish PR, Tsacopoulos M (2000) Mechanisms of glutamate metabolic signaling in retinal glial (Müller) cells. *J Neurosci* 20(5): 1809–1821.
50. Gordon GR, Choi HB, Rungta RL, Ellis-Davies GC, MacVicar BA (2008) Brain metabolism dictates the polarity of astrocyte control over arterioles. *Nature* 456(7223):745–749.
51. Pellerin L, Magistretti PJ (2012) Sweet sixteen for ANLS. *J Cereb Blood Flow Metab* 32(7):1152–1166.
52. Lauritzen KH, et al. (2014) Lactate receptor sites link neurotransmission, neurovascular coupling, and brain energy metabolism. *Cereb Cortex* 24(10):2784–2795.
53. Bozzo L, Puyal J, Chatton JY (2013) Lactate modulates the activity of primary cortical neurons through a receptor-mediated pathway. *PLoS One* 8(8):e71721.
54. Tang F, et al. (2014) Lactate-mediated glia-neuronal signalling in the mammalian brain. *Nat Commun* 5:3284.
55. Yang J, et al. (2014) Lactate promotes plasticity gene expression by potentiating NMDA signaling in neurons. *Proc Natl Acad Sci USA* 111(33):12228–12233.
56. Dirren E, et al. (2014) Intracerebroventricular injection of adeno-associated virus 6 and 9 vectors for cell type-specific transgene expression in the spinal cord. *Hum Gene Ther* 25(2):109–120.
57. Davidson S, Truong H, Nakagawa Y, Giesler GJ, Jr (2010) A microinjection technique for targeting regions of embryonic and neonatal mouse brain in vivo. *Brain Res* 1307: 43–52.
58. Jakoby P, et al. (2014) Higher transport and metabolism of glucose in astrocytes compared with neurons: A multiphoton study of hippocampal and cerebellar tissue slices. *Cereb Cortex* 24(1):222–231.
59. Hou BH, et al. (2011) Optical sensors for monitoring dynamic changes of intracellular metabolite levels in mammalian cells. *Nat Protoc* 6(11):1818–1833.
60. Tantama M, Hung YP, Yellen G (2012) Optogenetic reporters: Fluorescent protein-based genetically encoded indicators of signaling and metabolism in the brain. *Progress in Brain Research*, eds Knopfel T, Boyden E (Elsevier, Amsterdam), pp 235–263.
61. Barros LF, Baeza-Lehnert F, Valdebenito R, Ceballo S, Alegría K (2014) *Springer Protocols: Brain Energy Metabolism*, eds Waagepetersen HS, Hirrlinger J (Springer, Berlin).
62. San Martín A, et al. (2014) Single-cell imaging tools for brain energy metabolism: a review. *Neurophotonics* 1(1):011004.